Journal of Alloys and Compounds 508 (2010) 262–265

Contents lists available at ScienceDirect

Journal of Alloys and Compounds

journal homepage: www.elsevier.com/locate/jallcom

Luminescent properties of $Ca_{0.97}Al_2O_4:Eu_{0.01}^{2+},Dy_{0.02}^{3+}$ phosphors prepared by combustion method at different initiating temperatures

B.M. Mothudi*, O.M. Ntwaeaborwa*, Shreyas S. Pitale, H.C. Swart

Department of Physics, University of the Free State, P.O. Box 339, Bloemfontein, ZA 9300, South Africa

ARTICLE INFO

Article history:
Received 2 May 2010
Received in revised form 25 August 2010
Accepted 25 August 2010

Keywords:
Aluminates
Combustion method
Photoluminescence
Phosphorescence

ABSTRACT

$Ca_{0.97}Al_2O_4:Eu_{0.01}^{2+},Dy_{0.02}^{3+}$ powder phosphors were prepared by combustion method at different initiating temperatures (500–800 °C) using urea as a fuel. As confirmed by the X-ray diffraction (XRD) data, the powders crystallized in well known monoclinic phases of $CaAl_2O_4$, with traces of incidental impurities. Observed from the scanning electron microscopy (SEM) images were porous particles with irregular shapes and sizes and there were a lot of voids, which is a true reflection of the inherent nature of the combustion process. The PL spectra, recorded when the powders were excited by a 325 nm He–Cd laser at room temperature, showed broad blue emission with a maximum at 449 nm. This emission can be ascribed to $4f^65d^1$ to $4f^7$ transition of the Eu^{2+} ions. The maximum PL intensity was recorded from the sample prepared at the initiating temperature of 600 °C. Consistent with the PL emission data, the longer decay time was recorded from the same sample using Cary Eclipse spectrophotometer fitted with a monochromatized xenon lamp. The effect of initiating combustion temperature on the crystalline structure and PL intensity was investigated.

1. Introduction

Photoluminescence (PL) properties of Eu^{2+} doped alkaline earth aluminates phosphors with the general formula $MAl_2O_4:Eu^{2+}$ (M: Ca, Ba, Sr), have been studied extensively [1–5]. These phosphors have received a lot of attention due to their excellent luminescent properties, such as high luminescent intensity, high quantum efficiency and long-lasting phosphorescence [5]. The emission of Eu^{2+} can be tuned from blue to red depending on the host lattice. In addition the covalency, the size of the cation and the crystal field strength, seem to be other factors that influence the emission characteristics of Eu^{2+} in the host matrix [6,7]. It is well known that the afterglow lifetime and luminescence intensity can be enhanced by co-doping with a rare earth ion acting as a sensitizer [1]. Unlike the traditional green emitting ZnS:Cu phosphors, the $MAl_2O_4:Eu^{2+},Dy^{3+}$ phosphors are safer (because they are non-radioactive), chemically stable, and have long-lasting phosphorescence that leads to a large field of applications in luminous paints used in highway, airport escape routes, buildings, ceramic products and warning signs [5]. For example, $CaAl_2O_4:Eu^{2+},Nd^{3+}$ has been considered a useful violet emitting phosphor in luminous clocks and outdoor night time displays [8]. $CaAl_2O_4$ has a stuffed tridymite structure but transforms to at least three other polymorphs at high pressures [5]. In the stuffed tridymite structure there are two sites for the large cation, each with 9-fold coordination [5]. Zhong et al. [6] reported that the quality of the luminescent material is largely influenced by the synthesis technique. Over the years, $MAl_2O_4:Eu^{2+}$ (M = Ca, Sr, Ba) phosphors were mostly synthesized by high temperature solid-state and sol–gel methods, which require long reaction times. In recent years, the combustion method is preferred because of advantages such as low temperature shorter reaction, and reliability for preparation of long afterglow phosphors [6]. The objective for this study was to prepare a stable long afterglow blue phosphor, which may be used in infrastructure development. X-ray diffraction (XRD), scanning electron microscopy (SEM) and PL spectroscopy were used to investigate the influence of the initiating combustion temperature on the $CaAl_2O_4:Eu^{2+},Dy^{3+}$. The phosphorescent behavior of the phosphor is discussed based on the evaluation of decay characteristics.

2. Experimental

2.1. Synthesis

The powder samples of $Ca_{0.97}Al_2O_4:Eu_{0.01}^{2+},Dy_{0.02}^{3+}$, phosphors were synthesized at different initiating combustion temperatures. The following precursors: Calcium nitrate ($Ca(NO_3)_3{\cdot}4H_2O$), Aluminum nitrate ($Al(NO_3)_3{\cdot}9H_2O$), Europium nitrate ($Eu(NO_3)_3{\cdot}6H_2O$), Dysprosium nitrate ($Dy(NO_3)_3{\cdot}5H_2O$) and Urea ($CO(NH_2)_2$) all in analytical purity were weighed according to the stoichiometry. The precursors were mixed and milled in a mortar using a pestle, and a thick white paste was formed due to water of crystallization present on the metal nitrates. The resulting paste was then, divided into four portions, and was then introduced into a muffle

* Corresponding authors. Tel.: +27 51 401 2193; fax: +27 51 401 3507.
E-mail addresses: mothudibm@qwa.ufs.ac.za (B.M. Mothudi), ntwaeab@ufs.ac.za (O.M. Ntwaeaborwa).

0925-8388/$ – see front matter © 2010 Elsevier B.V. All rights reserved.
doi:10.1016/j.jallcom.2010.08.113

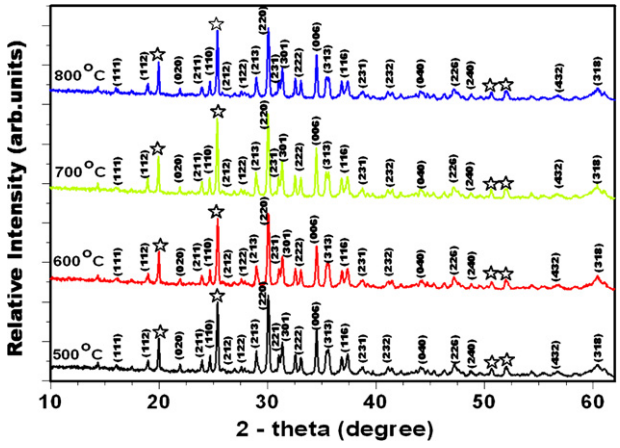

Fig. 1. XRD patterns of $Ca_{(0.97)}Al_2O_4:Eu_{0.01}{}^{2+},Dy_{0.02}{}^{3+}$ samples prepared at different initiating combustion temperatures.

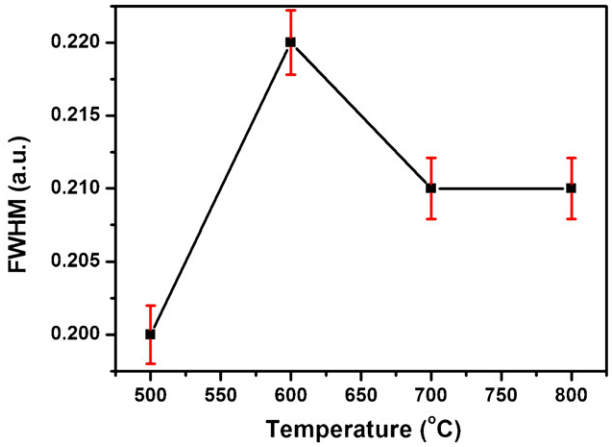

Fig. 2. Full width at half maximum (FWHM) for the 200 peak versus temperature.

furnace and the reaction was carried out at different initiating combustion temperatures ranging from 500 to 800 °C. The paste melted, underwent dehydration, and finally decomposed with the evolution of gases (oxides of nitrogen and ammonia). The mixture frothed and swelled, forming a foam that ruptured with a flame. The combustion process was completed in less than 5 min. The voluminous combustion ashes of the $Ca_{0.97}Al_2O_4:Eu_{0.01}{}^{2+},Dy_{0.02}{}^{3+}$, phosphors were grounded using a pestle and mortar to make fine powders. *Note* that the sintering process is not necessary for this method because the reducing atmosphere created during the reaction process is sufficient to change the ionization state of Eu^{3+} to Eu^{2+}.

2.2. Characterization

The crystalline structure, particle morphology and elemental composition of the phosphor powders were examined using a Panalytical X-ray diffractometer (XRD) with Cu Kα at λ = 1.5406 Å and Shimadzu Superscan SSX-550 scanning electron microscope (SEM) coupled with the energy dispersive X-rays spectrometer (EDS), respectively. A 325 nm He–Cd laser fitted with a SPEX 1870 (0.5 m spectrometer) and a photomultiplier tube detector was used to collect the PL data. The Cary Eclipse fluorescence spectrophotometer coupled with a monochromatized xenon lamp was used to analyze the phosphorescence properties of the phosphors. The PL data were collected in air at room temperature.

3. Results and discussion

Fig. 1 shows the XRD patterns of $CaAl_2O_4$ phosphors prepared at different initiating combustion temperatures. The main diffraction peaks indexed well with the monoclinic structure of $CaAl_2O_4$ according to JCPDS (70-0134) data file. There were additional impurity phases (marked with stars) that can be related to $CaAl_4O_7$ [8] or precursors that did not react completely during the combustion process. Similar impurity phases were also reported by Zhao and Chen [8] on $CaAl_2O_4:Eu^{2+},Nd^{3+}$ phosphors prepared at the initiating combustion temperatures of 400–600 °C. Haiyen et al. [9] reported that the presence of other impurity phases or some of the un-reacted precursors may be attributed to the fact that the combustion wave is not uniform and a portion of some of the precursors might not react completely in the process. It must also be noted that the small amount of doped rare earth ions has almost no effect on the $CaAl_2O_4$ phase composition. Singh et al. [10] reported similar XRD results when they prepared similar phosphors by the combustion method at an initiating combustion temperature of 600 °C. To evaluate the crystallinity of these phosphors, the full width at half maximum (FWHM) values were determined using the 220 peak and were plotted as a function of initiating temperatures as shown in Fig. 2. The FWHM increases with temperature from 0.2 (500 °C) to 0.22 (600 °C) and decreases to 0.21 at 700 and 800 °C. The data suggest that the highly crystalline $CaAl_2O_4$ was produced at the initiating temperature of 600 °C and the crystallinity decreased when the temperature was increased to 700 and 800 °C.

Fig. 3 shows the SEM morphology of the phosphor prepared by the combustion method at 600 °C. The non-uniform and irregular shapes of the particles shown in Fig. 2(a) illustrate the inherent nature of the combustion method. Singh et al. [11] ascribed the irregular particle shapes to the non-uniform distribution of temperature and mass flow in the combustion flame. The morphology of a porous product with the small particles close to the pores at higher resolution shown by Fig. 2(b) occurs during the combustion process when gases escape under high pressure. Although the samples were prepared at different initiating combustion temperatures, there were no significant variations on the surface morphologies of the phosphors.

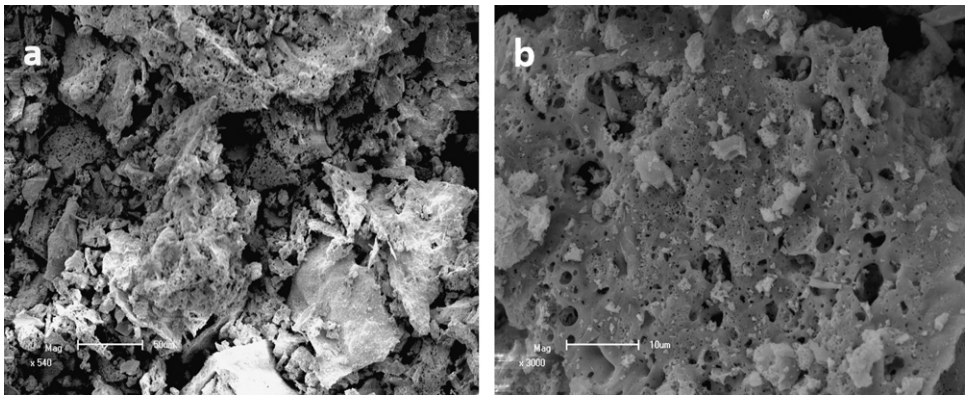

Fig. 3. SEM morphology of $Ca_{(0.97)}Al_2O_4:Eu_{0.01}{}^{2+},Dy_{0.02}{}^{3+}$ prepared at 600 °C.

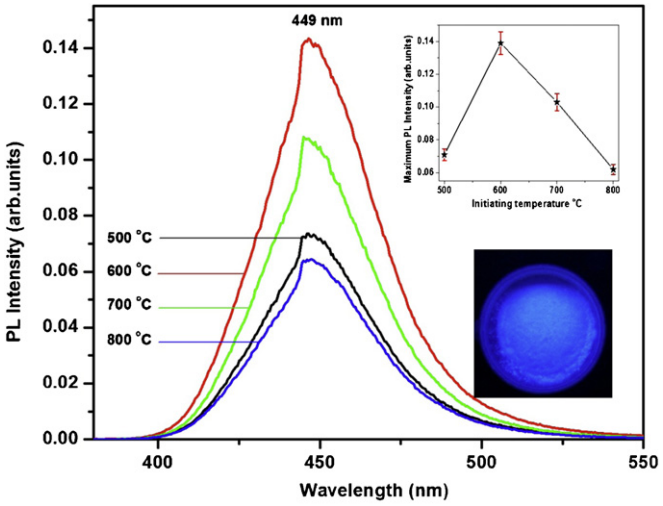

Fig. 4. PL emission spectra (λ_{exc} = 325 m) of the $Ca_{(0.97)}Al_2O_4:Eu_{0.01}{}^{2+},Dy_{0.02}{}^{3+}$ phosphor powder samples prepared at different initiating combustion temperatures, the maximum intensity versus temperature (with error bars) and a photograph the most intense powder captured when the powder was illuminated with a UV lamp.

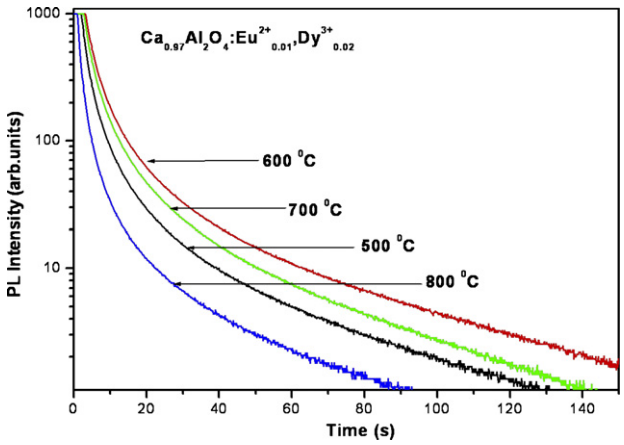

Fig. 5. Decay curves of $Ca_{(0.97)}Al_2O_4:Eu_{0.01}{}^{2+},Dy_{0.02}{}^{3+}$ phosphors prepared at different initiating combustion temperatures.

The PL emission spectra of $Ca_{(0.97)}Al_2O_4:Eu_{0.01}{}^{2+},Dy_{0.02}{}^{3+}$ phosphors prepared at different initiating combustion temperatures shown in Fig. 4 were excited by a 325 nm He–Cd laser at room temperature. The stable blue photoluminescence with a maximum at 449 nm was observed from all the phosphors. A photograph taken when the UV light was shone on the powder is shown in one of the insets of Fig. 4. This emission can be attributed to $4f^65d^1$ to $4f^7$ transition of the Eu^{2+} ion. The fact that the blue emission was stable at the same position suggests that changing the temperature did not affect radiative transitions in the Eu^{2+} ions and it also shows that there existed only one kind of luminescent centre. Similar results were reported by Chen et al. [12] and Park et al. [13] reported that there are three Ca^{2+} sites in the $CaAl_2O_4$ lattice, one is nine-coordinated and the others are six-coordinated by oxygen atoms. In the $CaAl_2O_4$ host lattice, Eu^{2+} ions prefer the nine-coordinated Ca^{2+} sites (rCa: 1.18 Å) to six-coordinated ones (rCa: 1.0 Å), because larger spaces are demanded for the substitution of Eu^{2+} ions (rEu: 1.30 Å) due to the ionic size difference [14]. The maximum intensity as a function of temperature is shown in the other inset of Fig. 4. The maximum PL intensity was observed from the sample prepared at 600 °C and the least intensity was observed from the sample prepared at 800 °C. As shown in Fig. 2, the sample prepared at 600 °C was more crystalline than the rest of the sample and hence more intense than the less crystalline samples. Poor crystallinity at 500 °C can be attributed to incomplete reaction of the precursors. On the other hand, igniting at temperatures ≥700 and 800 °C may lead to evolution of heat resulting in poorly crystalline phosphors and reduced PL intensity [15]. Yu et al. [15] prepared $SrAl_2O_4:Eu^{2+}$ at different initiating combustion temperatures ranging from 400 to 1000 °C, and the highest luminescent intensity was observed from the sample prepared at 600 °C. Liu et al. [16] reported an emission peak of 443 nm from $CaAl_2O_4:Eu^{2+},Dy^{3+}$ phosphors prepared at an initiating combustion temperature of 600 °C. As shown in Fig. 3, the initiating combustion temperature seems not to affect the position of the peaks, since all of them are symmetric at 449 nm. Similar results were reported by Yin et al. [17] from $CaTiO_3$:Pr,Al phosphors prepared at different initiating combustion temperatures.

Fig. 5 shows the decay curves of the samples after being irradiated with the monochromatized xenon lamp. As can be seen, the length of the decay time was consistent with the PL intensity, i.e. less intense phosphors decayed much faster than brighter phosphors. As shown in Table 1, the longest decay time was recorded from the brightest sample prepared at the initiating combustion temperature of 600 °C. Although the initiating temperature does not necessarily enhance the PL intensity or prolong the decay time, it plays an indirect role of improving crystallinity which in turn improves the general performance of the phosphor. This clearly shows that the initiating combustion temperature plays a major role when it comes to the luminescent properties of these phosphors. Yin et al. [17] investigated the effect of the initiating combustion temperature (500–900 °C) on the phosphorescence properties of $CaTiO_3$:Pr,Al phosphors and recorded the highest PL intensity from the sample prepared at the initiating combustion temperature of 800 °C and they attributed that to improved crystallinity at higher temperature.

In order to illustrate different decay times, the fittings of the decay profiles of the phosphors were calculated based on Eq. (1):

$$I = A_1 \exp\left(-\frac{t}{\tau_1}\right) + A_2 \exp\left(-\frac{t}{\tau_2}\right) + A_3 \exp\left(-\frac{t}{\tau_3}\right) \quad (1)$$

where I is the phosphorescence intensity at any time t after cutting off the UV excitation, A_1, A_2 and A_3 are constants and τ_1, τ_2 and τ_3 are decay times for the exponential components. The results in Table 1 confirm that the phosphor prepared at an initiating combustion temperature 600 °C has better afterglow properties than the other phosphors.

The fitted decay data of $Ca_{0.97}Al_2O_4:Eu_{0.01}{}^{2+},Dy_{0.02}{}^{3+}$ phosphor prepared at an initiating combustion temperature of 600 °C are shown in Fig. 6. The decay profiles of consisting of three exponential components, with different decay times designated exp 1, exp 2 and exp 3 are shown in the figure. The exp 1 parameter represents the rapid decay, which is due to the short survival time of the Eu^{2+} ion, the exp 2 parameter (intermediate transitional decay) is due to the capture of the Eu^{2+} by a shallow trap energy centre and exp 3 parameter (long-lasting phosphorescence) is the very long-lasting decay that could be attributed to the deep trap energy centre of Dy^{3+} [6]. The long persistence mechanism of the alkaline phosphors has been reported extensively by various researchers [6,18] and it is explained in terms of trapping and detrapping of charge carriers.

Table 1
Decay parameters of the phosphors calculated by curve fitting technique.

Phosphors	Temperature (°C)	τ_1 (s)	τ_2 (s)	τ_3 (s)
$Ca_{0.97}Al_2O_4:Eu_{0.01}{}^{2+},Dy_{0.02}{}^{3+}$	500	2.4	1.1	49.7
$Ca_{0.97}Al_2O_4:Eu_{0.01}{}^{2+},Dy_{0.02}{}^{3+}$	600	3.9	13.5	54.0
$Ca_{0.97}Al_2O_4:Eu_{0.01}{}^{2+},Dy_{0.02}{}^{3+}$	700	2.5	10.3	44.3
$Ca_{0.97}Al_2O_4:Eu_{0.01}{}^{2+},Dy_{0.02}{}^{3+}$	800	1.7	10.5	49.0

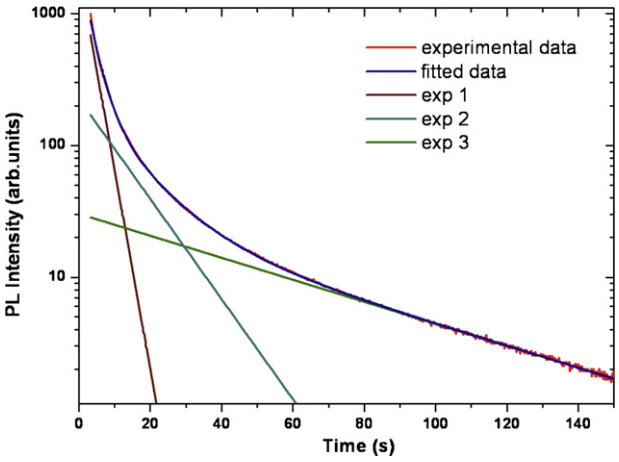

Fig. 6. Fitted decay data of the $Ca_{0.97}Al_2O_4:Eu_{0.01}^{2+},Dy_{0.02}^{3+}$ prepared at an initiating combustion temperature of 600 °C.

4. Conclusion

$Ca_{(0.97)}Al_2O_4:Eu_{0.01}^{2+},Dy_{0.02}^{3+}$ phosphors were successfully prepared by combustion method at different initiating temperatures. The monoclinic structures of $Ca_{(0.97)}Al_2O_4:Eu_{0.01}^{2+},Dy_{0.02}^{3+}$ were obtained at the different temperatures. The broad PL emission spectra for all the phosphors were symmetric at 449 nm, which confirms that the emitting centers remained at the fixed position. The influence of the initiating combustion temperature on crystallinity and hence photoluminescent intensity phosphors was investigated. The maximum intensity was observed from a highly crystalline phosphor prepared at 600 °C. The decay curves of the long persistent phosphors were fitted successfully using the three exponential decay times.

Acknowledgements

The SEM and X-ray diffractometer measurements were obtained from the Center of Microscopy (University of the Free State). This work was financially supported by the South African National Research Foundation (NRF). The funding for maintenance of the He–Cd laser at the Nelson Mandela Metropolitan University comes from research supported by the South African Chairs Initiative of the Department of the Science and Technology and National Research Foundation.

References

[1] H. Ryu, K.S. Bartwal, Physica B: Condens. Matter 403 (2008) 1843–1847.
[2] B.M. Mothudi, O.M. Ntwaeaborwa, J.R. Botha, H.C. Swart, Physica B: Condens. Matter 404 (2009) 4440–4444.
[3] O.M. Ntwaeaborwa, P.D. Nsimama, S. Pitale, I.M. Nagpure, V. Kumar, E. Coetsee, J.J. Terblans, P.T. Sechogela, H.C. Swart, J. Vac. Sci. Technol., A 28 (4) (2010) 901–905.
[4] B. Zhang, C. Zhao, D. Chen, Luminescence 25 (1) (2010) 25–29.
[5] G. Qiu, Y. Chen, X. Geng, L. Xiao, Y. Tian, Y. Sun, J. Rare Earths 23 (5) (2005) 629–632.
[6] H. Zhong, X. Zeng, S. Afr, J. Chem. 61 (2008) 22–25.
[7] R. Chen, Y. Wang, Y. Hu, Z. Hu, C. Liu, J. Lumin. 128 (2008) 1180–1184.
[8] C. Zhao, D. Chen, Mater. Lett. 61 (2007) 3673–3675.
[9] D. Haiyen, L. Gengshen, S. Jaiyue, J. Rare Earths 25 (2007) 19–22.
[10] V. Singh, T.K.G. Rao, D. Kim, Radiat. Meas. 43 (2008) 1198–1203.
[11] V. Singh, T.K.G. Rao, J. Zhu, J. Lumin. 128 (2008) 583–588.
[12] X.Y. Chen, C. Ma, X.X. Li, C.W. Shi, X.L. Li, D.R. Lu, J. Phys. Chem. C 113 (7) (2009) 2685–2689.
[13] Y.J. Park, Y.J. Kim, Mater. Sci. Eng., B 146 (2008) 84–88.
[14] T. Aitasalo, P. Deren, J. Hölsä, H. Jungner, M. Lastusaari, J. Niittykoski, Radiat. Meas. 38 (2004) 515–518.
[15] X. Yu, C. Zhou, X. He, Z. Peng, S. Yang, Mater. Lett. 58 (2004) 1087–1091.
[16] C. Liu, Y. Wang, Y. Hu, R. Chen, F. Liao, J. Alloys Compd. 470 (2009) 473–476.
[17] S. Yin, D. Chen, W. Tang, J. Alloys Compd. 441 (2007) 327–331.
[18] J.M. Ngaruiya, S. Nieuwoudt, O.M. Ntwaeaborwa, J.J. Terblans, H.C. Swart, Mater. Lett. 62 (2008) 3192–3194.